

This is the accepted manuscript made available via CHORUS, the article has been published as:

Influence of chemical doping on the magnetic properties of EuO

T. Mairoser, F. Loder, A. Melville, D. G. Schlom, and A. Schmehl

Phys. Rev. B **87**, 014416 — Published 11 January 2013

DOI: [10.1103/PhysRevB.87.014416](https://doi.org/10.1103/PhysRevB.87.014416)

Influence of Chemical Doping on the Magnetic Properties of EuO

T. Mairoser,^{*} F. Loder, and A. Schmehl

*Zentrum für Elektronische Korrelationen und Magnetismus,
Universität Augsburg, Universitätsstraße 1, 86159 Augsburg, Germany*

A. Melville

*Department of Materials Science and Engineering,
Cornell University, Ithaca, New York 14853, USA*

D. G. Schlom

*Department of Materials Science and Engineering,
Cornell University, Ithaca, New York 14853, USA and
Kavli Institute at Cornell for Nanoscale Science, Ithaca, New York 14853, USA*

(Dated: December 19, 2012)

Abstract

We report on the magnetic field dependence of the apparent **ferromagnetic ordering temperature** (T_F) of the ferromagnetic semiconductor EuO doped with 8% Gd, La, or Lu. Chemical doping is a common method to increase the T_F of EuO. Recent findings demonstrate that in thin films only a fraction of the dopants donate electrons into the conduction band. We show that the T_F of doped EuO determined by the standard procedure drastically increases with applied magnetic fields. The comparison of measured data to theoretical models is in agreement with large fractions of dopant electrons being localized and the presence of magnetic disorder.

PACS numbers: Valid PACS appear here

The ferromagnetic, half metallic semiconductor EuO (Curie temperature $T_C = 69\text{ K}$,¹ band gap $E_{\text{gap}} = 1.12\text{ eV}$ at 300 K) displays outstanding colossal magnetoresistive effects,³ metal-to-insulator transitions,⁴ magneto-optical effects,⁵ and close to 100% spin-polarization in the ferromagnetic state.^{6,7,8} Its ability to be epitaxially integrated with Si,⁷ GaN,⁷ and GaAs,⁹ render EuO a very promising material for spintronic applications. In addition, theoretical calculations predict highly strained EuO to become ferroelectric and even multiferroic.¹⁰ To make the outstanding physical properties of EuO of interest for more widespread use or even applications, the increase of its T_C is one of the main problems to be addressed. Rare earth doping with trivalent ions like La,^{7,8,11–13} Ce,¹⁴ Nd,¹² Sm,¹⁵ Gd,^{8,11,12,16–25} Ho,^{11,12} and Lu⁸ is the most commonly applied technique to increase T_C of EuO beyond its undoped value. This approach exploits an additional indirect exchange interaction, mediated via the conduction electrons supplied by the donors, that acts in addition to the direct Heisenberg exchange between the Eu $4f$ moments.^{26,27} Because of the simplicity of this approach, many doping studies have been performed on single crystals^{11,15–19} and thin films.^{8,12–14,20–25} Despite exploiting the same physical mechanism to increase T_C , the reported improvements vary strongly from experiment to experiment even for identical dopant elements and comparable dopant concentrations. These discrepancies might partially be explained by different magnetic background fields and different methods used to extract T_C from the magnetic data including several superconducting quantum interference device (SQUID) magnetometry-based methods, x-ray magnetic dichroism (XMCD), second harmonic generation (SHG), magneto-optic Kerr rotation, and neutron reflectometry (see table 1 for details). As EuO shows large magnetoresistive effects and a strong dependency of T_C on external magnetic fields, T_C derived at different magnetic background fields might not be comparable. In addition, recent findings show that in rare earth-doped EuO thin films a large fraction of the dopant atoms do not donate an electron into the conduction band and thereby limit the achievable increase in Curie temperature.^{8,23,24} A partial localization of the dopant electrons can explain this behavior and is in contrast to the assumptions on which theoretical models calculating the magnetic properties of doped EuO are based.^{26,27,34–36} In a rigorous sense, the term Curie temperature is only defined for a ferromagnetic phase transition at zero magnetic fields. Nevertheless, in the EuO community ferromagnetic ordering temperatures are regularly called Curie temperature, even when measured at substantial magnetic background fields. To avoid confusion, we use the term ferromagnetic ordering

Method	Applied Magnetic Field (G)	Reference
Magneto-optical Kerr rotation	***)	6
SQUID: onset of magnetization	0	7
SQUID: rise of derivation	1000	13
*) : derivation of magnetization	500	14
SQUID: **) and XMCD	100 and ***)	20
XMCD	***)	21
SQUID: **)	10	22
Neutron reflectometry	0, 125 or 250	28
SQUID: inflection point of $M(T)$	50	29
SHG	***)	30
SQUID: derivation of magnetization	10000	31
SQUID: **)	50	32
SQUID: linear fit to inverse of $M(T)$	2000	33

TABLE I: Measurement techniques for determining T_F of EuO. For the SQUID-based methods, the extraction methods of T_F from the data are listed. *) Measurement technique not named in the paper. **) Extraction method not provided. ***) Magnetic background field not given.

temperature (T_F) for measurements performed in non-zero magnetic background fields.

To address these questions and to provide a database for the comparison of experiments, in this Letter we investigate the dependence of T_F of 8% rare-earth-doped EuO ($\text{Eu}_{0.92}\text{B}_{0.08}\text{O}$, with $B = \text{Gd, La, Lu}$) on applied external magnetic fields. The doping concentration was chosen to be in the range of the maximum reported and theoretically predicted T_F values.^{15,16,21–23,26,27,34,35} The dopants were chosen to provide a spectrum of ionic radii, electron configurations, and to investigate possible differences between magnetic (Gd) and non-magnetic (La, Lu) dopants. To analyze systematically changes originating from applied external magnetic fields, we kept film thickness, microstructure, and oxygen content constant.

The films were grown using reactive oxide molecular-beam epitaxy (Veeco 930 and GEN10 MBE systems) on YAlO_3 single crystal substrates oriented within $\pm 0.5^\circ$ of (110).³⁷ Europium and the dopant elements were co-evaporated from effusion cells. The respective fluxes were calibrated to the desired Eu/dopant ratio using a quartz crystal microbalance. The total metal flux was set to $1.1 \times 10^{14} \text{ atoms/cm}^2\text{s}$. The films were deposited in O_2 partial pressures $P_{\text{O}_2} = 1.0 \times 10^{-9} \text{ Torr}$ above the vacuum chamber background pressure of $2 \times 10^{-9} \text{ Torr}$. To minimize additional charge carrier doping originating from oxygen vacancies, the films

were grown in the adsorption controlled growth regime at a substrate temperature of $T_{\text{sub}} = 350^\circ\text{C}$.^{24,37} To prevent their oxidation and to allow *ex situ* analysis, all films were capped with about 20 nm of amorphous silicon. After growth, *ex situ* four-circle x-ray diffraction (XRD) was used to characterize the structural quality of all films. The scans reveal epitaxial and single-phase films within the resolution limit of XRD. The high and comparable crystalline quality of all films is demonstrated by rocking curves on the 002 EuO peaks which show full width at half maximum of $\approx 0.01^\circ$. The in-plane magnetic properties of all films were determined using SQUID magnetometry.³⁸ To acquire the magnetic field dependence of the Curie temperature ($T_F(\mu_0 H)$), the temperature dependence of the film magnetization at a sequence of applied background fields ($M(T, H)$) was measured for all films.³⁸ The **ferromagnetic ordering temperatures** were extracted from the $M(T)$ data by taking the negative temperature derivative of the normalized magnetization ($-dM/dT(T)$). The high temperature shoulder of the peak associated with the onset of ferromagnetism was then defined as T_F . As it is the most commonly applied strategy within this approach, we chose to extract the T_F values by eye. The increasing uncertainty of this method at high fields is reflected in the respective error bars. A strict criterion for the T_F extraction could be introduced, but would be arbitrary and falsely suggest underlying physics and certainty which are not inherent to this method. To gain information about the dopant activation and to be able to compare the $M(T, H)$ data to theory, the transport properties and charge carrier densities n at 4.2 K of the rare earth-doped samples were measured using the Hall effect. For this, bridges were patterned into the films by the method described in Ref. 23.

Figure 1 shows the $M(T, H)$ characteristics of an 8% Gd-doped EuO film for applied fields $0 \leq \mu_0 H \leq 5$ T (a) and the respective theoretical results, calculated using Refs. 26 and 27 (b). For the theoretical calculations the measured charge carrier density $n = 9.0 \times 10^{20} \text{ cm}^{-3}$ was used as an input parameter. The corresponding $-dM/dT(T)$ characteristics are shown in Fig. 1(c) and 1(d). The derived **ferromagnetic ordering temperature** for every single measurement is shown in the supplemental materials.³⁸ Both, theory and experiment show a qualitatively similar behavior. The $M(T, H)$ data exhibit a shift from a sharp onset of ferromagnetism at zero field to broad and little defined transitions at high magnetic fields. This broadening makes the visual determination of T_F at high fields challenging. Only at low fields can sharp transitions be observed and utilized for the direct determination of T_F . The high temperature shoulders of the peaks in $-dM/dT(T)$ characteristics exhibit a systematic

shift to higher temperatures with increasing magnetic fields, which corresponds to an increase in the apparent T_F . The position of the peak maximum, however, stays almost constant at the value of the zero-field Curie temperature of the respective sample. The experimentally observed small shift of this peak is in agreement with the theoretical models, which were developed for Gd-doped EuO. The peak of $-dM/dT(T)$ is therefore suitable to extract comparable T_F s, despite the broadening at high fields. The corresponding uncertainty in the determination of T_F with increasing magnetic field is reflected in the respective error bars.

Despite the good qualitative agreement, theory and experiment differ quantitatively quite substantially, especially at low magnetic background fields. This is best demonstrated by comparing the $T_F(\mu_0 H)$ characteristics of the 8% Gd-doped EuO sample to the theoretical values (Fig. 2), both derived from the characteristics shown in Fig. 1.³⁸ At zero-field, the experimental Curie temperature of $T_C = 125$ K is lower than the theoretical value for $n = 9.0 \times 10^{20} \text{ cm}^{-3}$. The experimental $T_F(\mu_0 H)$ shows a more pronounced increase at low fields and settles into a steady, but less steep slope at higher magnetic fields. The steeper slope of the experimental $T_F(\mu_0 H)$ characteristics at high fields thereby leads to a gradual reduction of the T_F difference between theory and experiment. These differences between experiment and theory are explained by the unjustified assumption of a totally unperturbed lattice of magnetic ions, just like in undoped EuO. This is a good assumption with respect to the $4f^7$ electron configuration of Gd^{3+} , which is identical to that of Eu^{2+} . Nevertheless, one can expect that the incorporation of a high amount of doping impurities will cause local structural as well as magnetic disorder. As the magnetic disorder should be suppressed by the application of an external magnetic field, the discrepancy between theory and experiment is reduced, as observed. We also point out, that the measured charge carrier density of $n = 9.0 \times 10^{20} \text{ cm}^{-3}$ for 8% Gd-doped EuO corresponds to only 30% of the Gd ions donating an electron into the conduction band. In our case, a theoretical calculation based on the widespread assumption of 100% dopant activation would therefore grossly overestimate the charge carrier density and deviate completely from the experimental data (Fig. 2), because the highest T_C in the model is reached for $n \approx 10^{21} \text{ cm}^{-3}$.^{26,27} This emphasizes the necessity to base the comparison between experimental data and theory on measured carrier densities rather than on dopant concentrations.

Effects originating from magnetic disorder and the influence of different doping elements

can systematically be investigated by replacing the magnetic Gd^{3+} ions ($5p^6 4f^7$) by non-magnetic Lu^{3+} ($5p^6 4f^{14}$) or La^{3+} ($5p^6 4f^0$). The latter dopants are expected to donate electrons into the conduction band just like Gd, inducing an indirect exchange interaction increasing T_C . On the other hand, they also cause a weakening of the direct exchange between the rare earth ions, leading to a suppression of T_C . The combined strength of these two exchange mechanisms determines the actual Curie temperature of each individual sample. Fig. 3 shows the $T_F(\mu_0 H)$ characteristics of EuO films doped with 8% La-, Lu-, or Gd, together with the theoretical values of Fig. 2.³⁸ All three doped samples show comparable zero-field Curie temperatures and carrier densities, with $T_{C,\text{Gd}} = 125 \text{ K}$ ($n_{\text{Gd}} = 9.0 \times 10^{20} \text{ cm}^{-3}$), $T_{C,\text{La}} = 116 \text{ K}$ ($n_{\text{La}} = 1.1 \times 10^{21} \text{ cm}^{-3}$), and $T_{C,\text{Lu}} = 126 \text{ K}$ ($n_{\text{Lu}} = 2.1 \times 10^{20} \text{ cm}^{-3}$). The La-doped EuO sample behaves most like the Gd-doped one. Despite its larger carrier density, it shows systematically lower **ferromagnetic ordering temperatures**, which can be attributed to the reduced direct Heisenberg exchange. The low field gain in **ferromagnetic ordering temperature** ($T_F(1 \text{ T})/T_C(0 \text{ T})$) is slightly more pronounced for La (129%) as for Gd (120%), indicating greater magnetic disorder in the La-doped sample. The slopes of $T_F(\mu_0 H)$ at high fields are again very similar. A much more pronounced difference is observed in the $T_F(\mu_0 H)$ data of the 8% Lu-doped EuO film. Despite having a much smaller charge carrier density and dopant activation, its zero-field Curie temperature is close to that of the Gd-doped film. Compared to the La- and Gd-doped samples, the Lu-doped film shows a much stronger increase at low field ($T_F(1 \text{ T})/T_C(0 \text{ T}) = 142\%$). Above 1 T, the slopes of the $T_F(\mu_0 H)$ characteristics are again very similar for all three doped samples. Nevertheless, the steep initial increase leads to a much stronger overall gain of $T_F(5 \text{ T})/T_C(0 \text{ T})$ of about 170% for Lu as compared to 154% and 159% for Gd and La, respectively. These findings, a high T_F despite a low n and a larger overall T_F increase with applied field, indicate that in addition to charge carrier density and magnetic disorder, additional influences such as film microstructure, dopants size,²⁵ and electron configuration might play a role in determining the Curie temperature of rare earth-doped EuO.

In conclusion, we have investigated the magnetic field dependence of the **ferromagnetic ordering temperatures** of 8% Gd-, La-, or Lu-doped EuO films and compared it to a theoretical model developed for Gd-doped EuO. Using measured charge carrier densities as input parameters for the calculations, the experimental and theoretical Curie temperatures at high field of Gd-doped EuO are in good agreement. At low fields, however, theory tends

to overestimate T_C . This behavior is in agreement with the presence of magnetic disorder in the samples, which is not accounted for in the theoretical models. This behavior is even more pronounced, if the magnetic dopant Gd^{3+} is replaced by the non-magnetic ions La^{3+} and Lu^{3+} . Strong T_F increases at low fields are followed by comparable $T_F(\mu_0 H)$ slopes at high fields for all three dopants. The large observed quantitative difference between the La- and Lu-doped EuO indicates the presence of additional influences determining T_F . Furthermore, the measured charge carrier densities demonstrate that only a fraction of the introduced dopants transfer electrons into the EuO conduction band. A refined theory describing the doping and magnetic-field dependence of the Curie temperature of EuO should therefore include the influences of low dopant activity and of structural and magnetic disorder. In addition, the presented data demonstrates that T_F , determined at even moderate magnetic background fields, tend to largely overestimate the intrinsic T_C of the doped EuO samples. The determination of T_C at zero applied field is therefore preferable.

We gratefully acknowledge C. Richter for doing some of the calculations. The work in Augsburg was supported by the DFG (Grant No. TRR 80) and the EC (oxIDes). The work at Cornell was supported by the AFOSR (Grant No. FA9550-10-1-0123). AM gratefully acknowledges support from the NSF IGERT program (NSF Award DGE-0654193) and by the IMI Program of the National Science Foundation under Award No. DMR 0843934.

* thomas.mairoser@physik.uni-augsburg.de

- ¹ T. R. McGuire and M. W. Shafer, J. Appl. Phys. **35**, 984 (1964).
- ² J. O. Dimmock, IBM J. Res. Dev. **14**, 301 (1970).
- ³ Y. Shapira, S. Foner, and T. B. Reed, Phys. Rev. B **8**, 2299 (1973).
- ⁴ G. Petrich, S. von Molnár, and T. Penney, Phys. Rev. Lett. **26**, 885 (1971).
- ⁵ K. Y. Ahn, and J. C. Suits, IEEE Trans. Magnetics **3**, 453 (1967).
- ⁶ P. G. Steeneken, L. H. Tjeng, I. Elfimov, G. A. Sawatzky, G. Ghiringhelli, N. B. Brookes, and D.-J. Huang, Phys. Rev. Lett. **88**, 047201 (2002).
- ⁷ A. Schmehl, V. Vaithyanathan, A. Herrnberger, S. Thiel, C. Richter, M. Liberati, T. Heeg, M. Röckerath, L. F. Kourkoutis, S. Mühlbauer, P. Böni, D. A. Muller, Y. Barash, J. Schubert, Y. Idzerda, J. Mannhart, and D. G. Schlom, Nat. Mater. **6**, 882 (2007).
- ⁸ A. Melville, T. Mairoser, A. Schmehl, D. E. Shai, E. J. Monkman, J. W. Harter, T. Heeg, B. Holländer, J. Schubert, K. M. Shen, J. Mannhart, and D. G. Schlom, Appl. Phys. Lett. **100**, 222101 (2012).
- ⁹ A. G. Swartz, J. Ciraldo, J. J. I. Wong, Y. Li, W. Han, T. Lin, S. Mack, J. Shi, D. D. Awschalom, and R. K. Kawakami, Appl. Phys. Lett. **97**, 112509 (2010).
- ¹⁰ E. Bousquet, N. A. Spaldin, and P. Ghosez, Phys. Rev. Lett **104**, 037601 (2010).
- ¹¹ M. W. Shafer and T. R. McGuire, J. Appl. Phys. **39**, 588 (1968).
- ¹² K. Y. Ahn and T. R. McGuire, J. Appl. Phys. **39**, 5061 (1968).
- ¹³ H. Miyazaki, H. J. Im, K. Terashima, S. Yagi, M. Kato, K. Soda, T. Ito, and S. Kimura, Appl. Phys. Lett. **96**, 232503 (2010).
- ¹⁴ P. Liu, J. Tang, J. A. Colón Santana, K. D. Belashchenko, and P. A. Dowben, J. Appl. Phys. **109**, 07C311 (2011).
- ¹⁵ A. A. Samokhvalov, T. I. Arbuzova, V. S. Babushkin, B. A. Gizhevskii, N. N. Efremova, M. I. Simonova, and N. M. Chebotaev, Sov. Phys. Solid State **18**, 1655 (1976).
- ¹⁶ A. A. Samokhvalov, B. A. Gizhevskii, M. I. Simonova, and N. I. Solin, Sov. Phys. Solid State **14**, 230 (1972).
- ¹⁷ A. A. Samokhvalov T. I. Arbuzova, M. I. Simonova, L. D. Fal'kovskaya, Sov. Phys. Solid State **16**, 2459 (1974).

- ¹⁸ C. Godart, A. Mauger, J. P. Desfours, and J. C. Achard, J. Phys. Colloques **41**, C5-219 (1980).
- ¹⁹ A. Mauger, M. Escorne, C. Godart, J. P. Desfours, and J. C. Achard, J. Phys. Colloques **41**, C5-263 (1980).
- ²⁰ T. Matsumoto, K. Yamaguchi, M. Yuri, K. Kawaguchi, N. Koshizaki, and K. Yamada, J. Phys.: Condens. Matter **16**, 6017 (2004).
- ²¹ H. Ott, S. J. Heise, R. Sutarto, Z. Hu, C. F. Chang, H. H. Hsieh, H.-J. Lin, C. T. Chen, and L. H. Tjeng, Phys. Rev. B **73**, 094407 (2006).
- ²² R. Sutarto, S. G. Altendorf, B. Coloru, M. Moretti Sala, T. Haupricht, C. F. Chang, Z. Hu, C. Schüßler-Langeheine, N. Hollmann, H. Kierspel, J. A. Mydosh, H. H. Hsieh, H.-J. Lin, C. T. Chen, and L. H. Tjeng, Phys. Rev. B **80**, 085308 (2009).
- ²³ T. Mairoser, A. Schmehl, A. Melville, T. Heeg, L. Canella, P. Böni, W. Zander, J. Schubert, D. E. Shai, E. J. Monkman, K. M. Shen, D. G. Schlom, and J. Mannhart, Phys. Rev. Lett. **105**, 257206 (2010).
- ²⁴ T. Mairoser, A. Schmehl, A. Melville, T. Heeg, W. Zander, J. Schubert, D. E. Shai, E. J. Monkman, K. M. Shen, T. Z. Regier, D. G. Schlom, and J. Mannhart, Appl. Phys. Lett. **98**, 102110 (2011).
- ²⁵ S. G. Altendorf, N. Hollmann, R. Sutarto, C. Caspers, R. C. Wicks, Y.-Y. Chin, Z. Hu, H. Kierspel, I. S. Elfimov, H. H. Hsieh, H.-J. Lin, C. T. Chen, and L. H. Tjeng, Phys. Rev. B **85**, 081201 (2012).
- ²⁶ A. Mauger, Phys. Status Solidi B **84**, 761 (1977).
- ²⁷ S. Burg, V. Stukalov, and E. Koganm, Phys. Status Solidi B **249**, 847 (2012).
- ²⁸ S. Mühlbauer, P. Böni, R. Georgii, A. Schmehl, D. G. Schlom, and J. Mannhart, J. Phys. Condens. Matter **20**, 104230 (2008).
- ²⁹ M. Müller, G.-X. Miao, and J. S. Moodera, J. Appl. Phys. **105**, 07C917 (2009).
- ³⁰ M. Matsubara, A. Schmehl, J. Mannhart, D. G. Schlom, and M. Fiebig, Phys. Rev. B **81**, 214447 (2010).
- ³¹ M. Barbagallo, N. D. M. Hine, J. F. K. Cooper, N.-J. Steinke, A. Ionescu, C. H. W. Barnes, C. J. Kinane, R. M. Dalgliesh, T. R. Charlton, and S. Langridge, Phys. Rev. B **81**, 235216 (2010).
- ³² M. Barbagallo, T. Stollenwerk, J. Kroha, N.-J. Steinke, N. D. M. Hine, J. F. K. Cooper, C. H. W. Barnes, A. Ionescu, P. M. D. S. Monteiro, J.-Y. Kim, K. R. A. Ziebeck, C. J. Kinane, R. M. Dalgliesh, T. R. Charlton, and S. Langridge, Phys. Rev. B **84**, 075219 (2011).

- ³³ T. Yamasaki, K. Ueno, A. Tsukazaki, T. Fukumura, and M. Kawasaki, Appl. Phys. Lett. **98**, 082116 (2011).
- ³⁴ M. Arnold and J. Kroha, Phys. Rev. Lett. **100**, 046404 (2008).
- ³⁵ N. J. C. Ingle and I. S. Elfimov, Phys. Rev. B **77**, 121202 (2008).
- ³⁶ H. Wang, C. Schuster, and U. Schwingenschlögl, Chem. Phys. Lett. **524**, 68 (2012).
- ³⁷ R. W. Ulbricht, A. Schmehl, T. Heeg, J. Schubert, and D. G. Schlom, Appl. Phys. Lett. **93**, 102105 (2008).
- ³⁸ See the supplementary information section of this paper for details.
- ³⁹ R. Chartrand, ISRN Appl. Math. **2011**, 164564 (2011).

Captions:

Figure 1: (a) normalized measured temperature dependence of the magnetization $M(T, H)$ of a $\text{Eu}_{0.92}\text{Gd}_{0.08}\text{O}$ sample at different external magnetic fields $\mu_0 H$; (b) calculated $M(T, H)$ characteristics of Gd doped EuO at $n = 9.0 \times 10^{20} \text{ cm}^{-3}$ according to Refs. 26 and 27; (c) $-dM/dT(T)$ characteristics derived from the data shown in (a) calculated using the algorithm described in Ref. 39 for $\alpha = 0.25$; (d) $-dM/dT(T)$ characteristics derived from the data shown in (b).

Figure 2: Magnetic field dependence of T_F of a $\text{Eu}_{0.92}\text{Gd}_{0.08}\text{O}$ sample (red curve with circles) compared to the respective theoretical values for $n = 9.0 \times 10^{20} \text{ cm}^{-3}$ (blue curve with squares) and the nominal carrier density $n = 2.4 \times 10^{21} \text{ cm}^{-3}$ for 100% active dopants (orange curve with triangles) according to Refs. 26 and 27. The T_F values are derived from the $-dM/dT(T)$ data shown in Fig. 1. The solid curves are guides for the eye.

Figure 3: Magnetic field dependence of T_F of a $\text{Eu}_{0.92}\text{La}_{0.08}\text{O}$ sample (light blue curve with rhombi), a $\text{Eu}_{0.92}\text{Lu}_{0.08}\text{O}$ sample (orange curve with triangles), $\text{Eu}_{0.92}\text{Gd}_{0.08}\text{O}$ (red curve with circles), and the respective theoretical values calculated for $n = 9.0 \times 10^{20} \text{ cm}^{-3}$ according to Refs. 26 and 27 (blue curve with squares). The solid curves are guides for the eye.

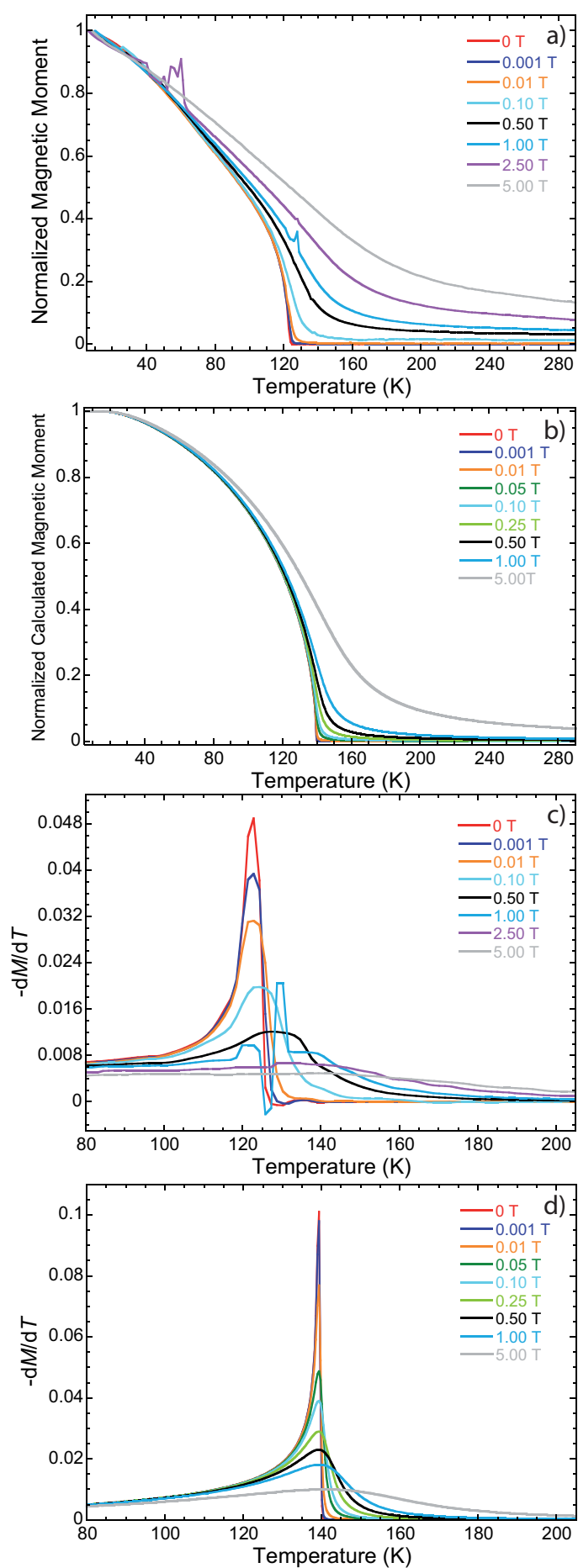


Figure 1

XXXXXXXX

19Dec2012

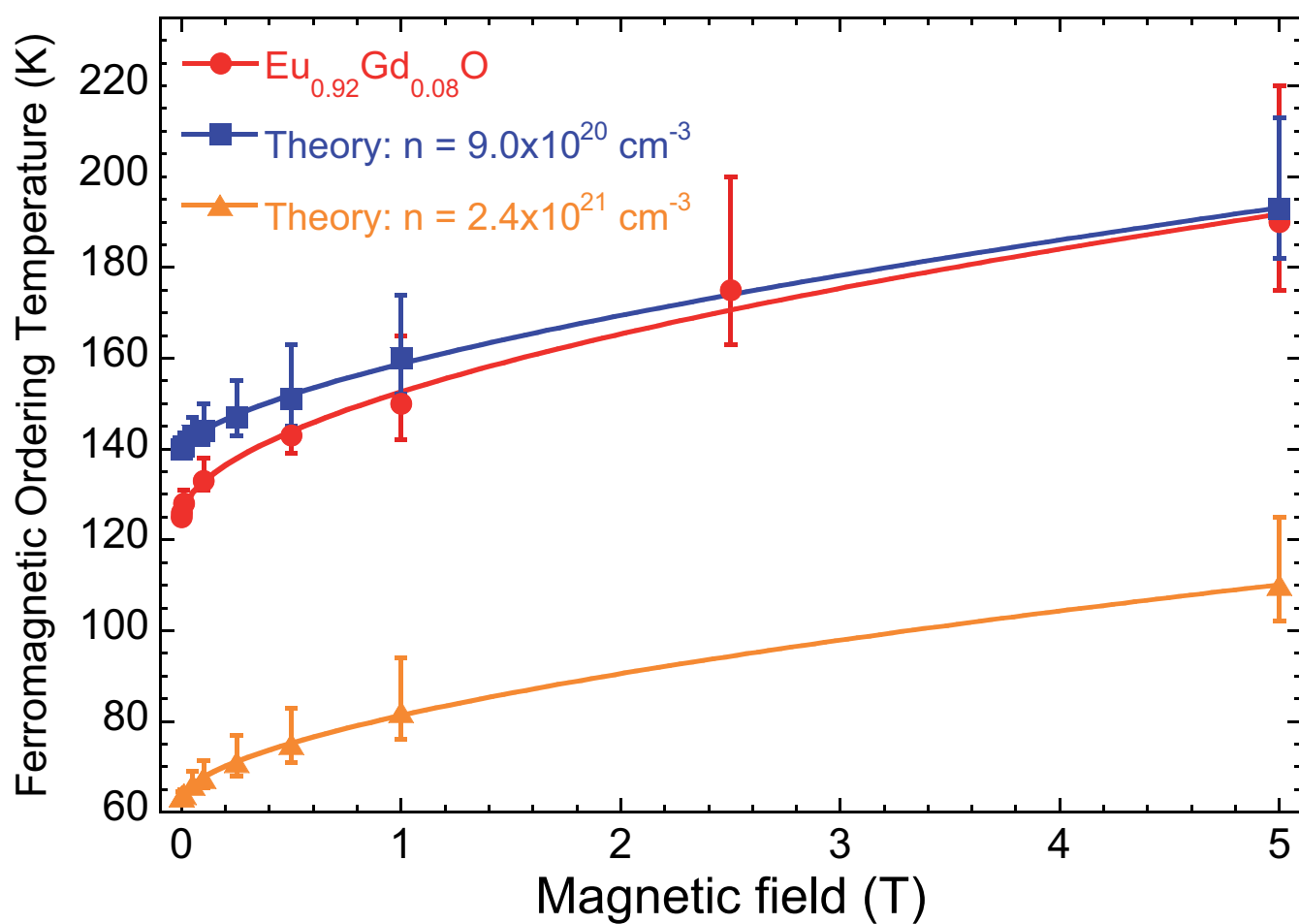


Figure 2

XXXXXXXX

19Dec2012

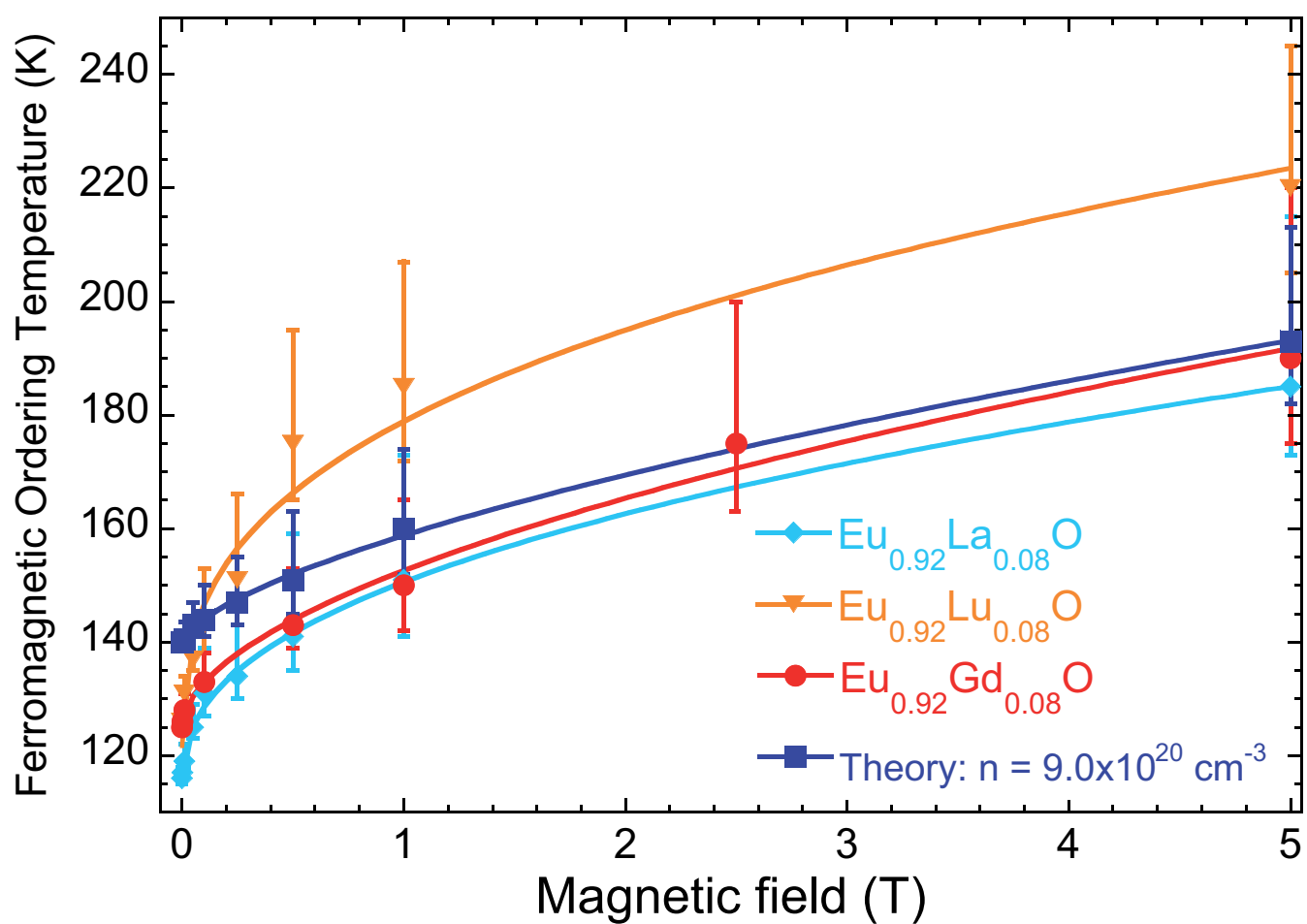


Figure 3

XXXXXXXXX

19Dec2012